

Review

Dynamics and Geometry of Icosahedral Order in Liquid and Glassy Phases of Metallic Glasses

Masato Shimono * and Hidehiro Onodera

National Institute for Materials Science, 1-2-1 Sengen, Tsukuba 305-0047, Japan;

E-Mail: onodera.hidehiro@nims.go.jp

* Author to whom correspondence should be addressed; E-Mail: shimono.masato@nims.go.jp;
Tel.: +81-29-860-4965; Fax: +81-02-860-4960.

Academic Editors: Jordi Sort Viñas and K. C. Chan

Received: 22 May 2015 / Accepted: 25 June 2015 / Published: 2 July 2015

Abstract: The geometrical properties of the icosahedral ordered structure formed in liquid and glassy phases of metallic glasses are investigated by using molecular dynamics simulations. We investigate the Zr-Cu alloy system as well as a simple model for binary alloys, in which we can change the atomic size ratio between alloying components. In both cases, we found the same nature of icosahedral order in liquid and glassy phases. The icosahedral clusters are observed in liquid phases as well as in glassy phases. As the temperature approaches to the glass transition point T_g , the density of the clusters rapidly grows and the icosahedral clusters begin to connect to each other and form a medium-range network structure. By investigating the geometry of connection between clusters in the icosahedral network, we found that the dominant connecting pattern is the one sharing seven atoms which forms a pentagonal bicap with five-fold symmetry. From a geometrical point of view, we can understand the mechanism of the formation and growth of the icosahedral order by using the Regge calculus, which is originally employed to formulate a theory of gravity. The Regge calculus tells us that the distortion energy of the pentagonal bicap could be decreased by introducing an atomic size difference between alloying elements and that the icosahedral network would be stabilized by a considerably large atomic size difference.

Keywords: metallic glasses; icosahedral order; medium-range order; molecular dynamics simulation; glass-forming ability; Regge calculus

1. Introduction

Icosahedral symmetry is considered to play an important role in the atomic scale structure of glassy phases in spherically interacting systems. The Dense Random Packing (DRP) model was proposed by Bernal for liquid phases in his pioneering work [1], and was later applied to a structure of amorphous metals [2]. In this model, the icosahedral cluster formed by 13 atoms located at the center and the 12 vertices of an icosahedron is a key building block and is basis of the icosahedral short-range order in liquid and glassy phases. The early works of computer simulation have shown that the icosahedral order would exist in both liquid and glassy phases [3,4]. After the discovery of good metallic glass-formers [5,6], experimental observations [7–12] has reported that the icosahedral short-range order does exist in metallic glasses and that some medium-range order may also exist beyond the icosahedral short-range order. However, it was little known how the icosahedral short-range order is arranged and extended to form a medium-range order in glassy phases. In other words, the interrelation between the icosahedral clusters was not clear. In recent years, two milestone models for icosahedral medium-range structure have been proposed: One is the fcc packing of icosahedral clusters proposed by Miracle [13] and the other is the icosahedral packing of icosahedral clusters and the strings of connected of icosahedra proposed by Sheng *et al.* [14]. Being enlightened to these models, a family of network-type models has been proposed with a special attention on the bonding topology between icosahedral clusters, such as the “bicap sharing” (or “interpenetrating” depending on authors) network [15–17], the string-like backbone network [18,19], and the superclusters [20,21]. Especially, Ding *et al.* have elegantly shown [22] that the icosahedral order can be generally understood as the polyhedral packing by the Frank-Kasper polyhedra [23], which are formulated based on the notion of DRP and include the icosahedron as a member. In addition, recent experimental observations [24] and simulation studies [25,26] have revealed that the icosahedral network formation is closely related to the “slowing down” of the relaxation dynamics in supercooled liquids near the glass transition. Despite the understanding of the nature of icosahedral order is gradually deepened in both structural and dynamical aspects, the physics behind the formation of the icosahedral medium-range order is not fully understood yet. In the present study, we investigate geometrical and dynamical properties of the icosahedral order formed in both liquid and glassy phases of metallic glasses by using molecular dynamics (MD) simulations.

MD simulation is a method to calculate the moving trajectories of atoms by solving the Newtonian equations of motion numerically. It is a powerful tool to investigate the atomic scale structure because all information of atomic configurations can be drawn at any time in the course of calculations. Since the purpose of our study is to clarify the geometrical nature underlying the icosahedral medium-range ordered structure formed in glassy phases and supercooled liquid phases of metallic glasses, the MD technique is highly useful. This article is planned as follows. The methods of MD simulation are given in Section 2. Section 3 is devoted to the simulation results and discussion. The results for the Zr-Cu system are shown in Subsection 3.1, the results for a model alloy system are shown in Subsection 3.2, and the Regge calculus is introduced in Subsection 3.3 to discuss the geometrical properties of the icosahedral ordered structure found in the simulations. The conclusion is given in Section 4.

2. Methods

2.1. Interatomic Potentials

In the classical molecular dynamics simulations, interatomic potentials between constituent atoms play a decisive role in the calculation. In this study, we use two different types of potentials: One is a many-body potential [27] based on the electron density theory for the Zr-Cu system, and the other is a two-body potential [28] for a model alloy system.

For the Zr-Cu system, we use a many-body Finnis-Sinclair type potential [27] developed by Rosato *et al.* [29], which has a functional form as

$$V_i = -\sqrt{\rho_i} + \sum_j \phi_{ij} \quad (1)$$

$$\phi_{ij}(r_{ij}) = A_{ij} \exp p_{ij}(1 - r_{ij} / r_{ij}^0) \quad (2)$$

$$\rho_i(r_{ij}) = \sum_j \xi_{ij}^2 \exp 2q_{ij}(1 - r_{ij} / r_{ij}^0) \quad (3)$$

where r_{ij} is the distance between atoms i and j and the parameters p_{ij} , q_{ij} , A_{ij} , ξ_{ij} and r_{ij}^0 are determined by us [30] to reproduce the mixing enthalpy of the Zr-Cu system and the lattice parameters, elastic moduli and the cohesive energies of hcp-Zr, fcc-Cu, and the B2-ZrCu phase.

It is well known that the atomic size ratio between the constituent elements plays an important role in the formation of metallic glasses [31]. Therefore, for a simple model for binary alloys, we assume the interaction between atoms i and j to be described by the 8-4 type Lennard-Jones potential [28] V^{ij} as

$$V^{ij}(r) = e_0^{ij} \left\{ \left(r_0^{ij} / r \right)^8 - 2 \left(r_0^{ij} / r \right)^4 \right\} \quad (4)$$

The merit of using this potentials is that we can independently vary the atomic size and the chemical bond strength by changing the parameters r_0^{ij} and e_0^{ij} , respectively. In this study, to focus on the atomic size effect, we assume for a binary system composed of elements A and B as $r_0^{AA} = 1$, $r_0^{BB} \leq 1$, $r_0^{AB} = (r_0^{AA} + r_0^{BB})/2$, and $e_0^{AA} = e_0^{BB} = e_0^{AB} = 1$. Thus, we can vary the atomic size ratio r_0^{BB} of the element B to A, and the concentration x_B of the smaller element B. The atomic masses of both elements are also supposed to be the same unit mass. All physical quantities are expressed in the above units for the model system.

2.2. Simulation Procedure

The simulation system consists of 4000 to 16,000 atoms, and is confined in a cubic simulation cell with periodic boundary conditions imposed in all three directions. The temperature of the system is controlled by scaling the atomic momenta. The pressure of the system is kept zero by changing the size of the simulation cell according to the constant pressure formalism [32].

In the simulation the alloy system is started from a liquid phase above the melting point and quenched down to solidify, which brings us a glassy phase or a crystalline phase depending on the cooling rate. After a glassy phase is produced, the system is heated up again and kept at a constant temperature for isothermal annealing, if needed. By monitoring the volume, energy, radial distribution of atoms, and the atomic diffusion, we can detect the phase properties at any stage.

2.3. Icosahedral Symmetry

We shall investigate the local atomic structure of liquid and glassy phases with paying a special attention to the icosahedral symmetry. For this purpose, we use the Voronoi tessellation analysis [1], in which the local symmetry around each atom is indexed by a set of integers (n_3, n_4, n_5, n_6) , where n_i is the number of i -edged faces of the Voronoi cell. By calculating this index for each atom, we define the icosahedral cluster by the atom that has the Voronoi index $(0, 0, 12, 0)$ and its neighbors.

3. Results and Discussion

3.1. Icosahedral Order in Zr-Cu System

3.1.1. Icosahedral Medium-range Order in Zr-Cu Metallic Glasses

Firstly we examine the icosahedral order in glassy phases of the Zr-Cu alloys. Figure 1 shows all icosahedral clusters picked up by the Voronoi analysis found in an as-quenched $N = 8000$ Zr₄₀Cu₆₀ glassy phase. To investigate the medium-range order or the interrelation between the icosahedral clusters, we also calculate the Voronoi indices between the icosahedral clusters. Unfortunately, we could not detect any signature of fcc order or icosahedral order of the clusters, but found an inhomogeneous and string-like [14,18] network structure as shown in Figure 1. To characterize the topological nature of this network, we check the connecting pattern between adjacent clusters.

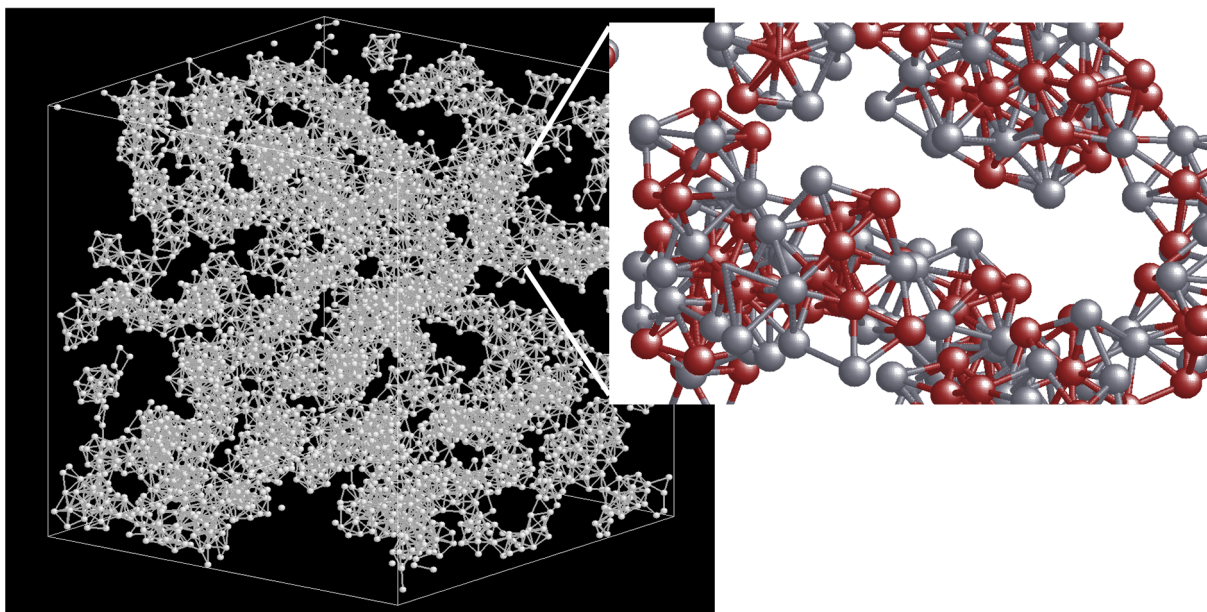


Figure 1. Snapshot of icosahedral clusters formed in an as-quenched Zr₄₀Cu₆₀ glassy phase. In the inset, the gray and brown spheres denote the Zr and Cu atoms.

3.1.2. Geometrical Feature of Icosahedral Network

When two icosahedral clusters are linked together, the linking patterns can be classified into the following four types [15] as illustrated in Figure 2: (1) Vertex sharing, where one atom is shared by two clusters; (2) edge sharing, where two atoms forming a link are shared; (3) face sharing, where three

atoms forming a triangle are shared; and (4) bicap sharing, where seven atoms forming a pentagonal bicap are shared or two icosahedra are interpenetrating each other. We have counted the population of these four linking patterns for an as-quenched $N = 8000$ $Zr_{40}Cu_{60}$ glassy phase. The results are shown in Figure 2, where the population of the isolated and the linked icosahedral clusters are also shown as well as the population of vertex sharing, the edge sharing, the face sharing, and the bicap sharing connection. We can see that the network mainly consists of bicap sharing connection and this type of connection should be a key to understand the medium-range order in metallic glasses. It is consistent with the recent experimental observation [12] by the scanning electron nanodiffraction that suggests a face sharing or bicap sharing model of the icosahedral medium-range order in a $Zr_{36}Cu_{64}$ glass.

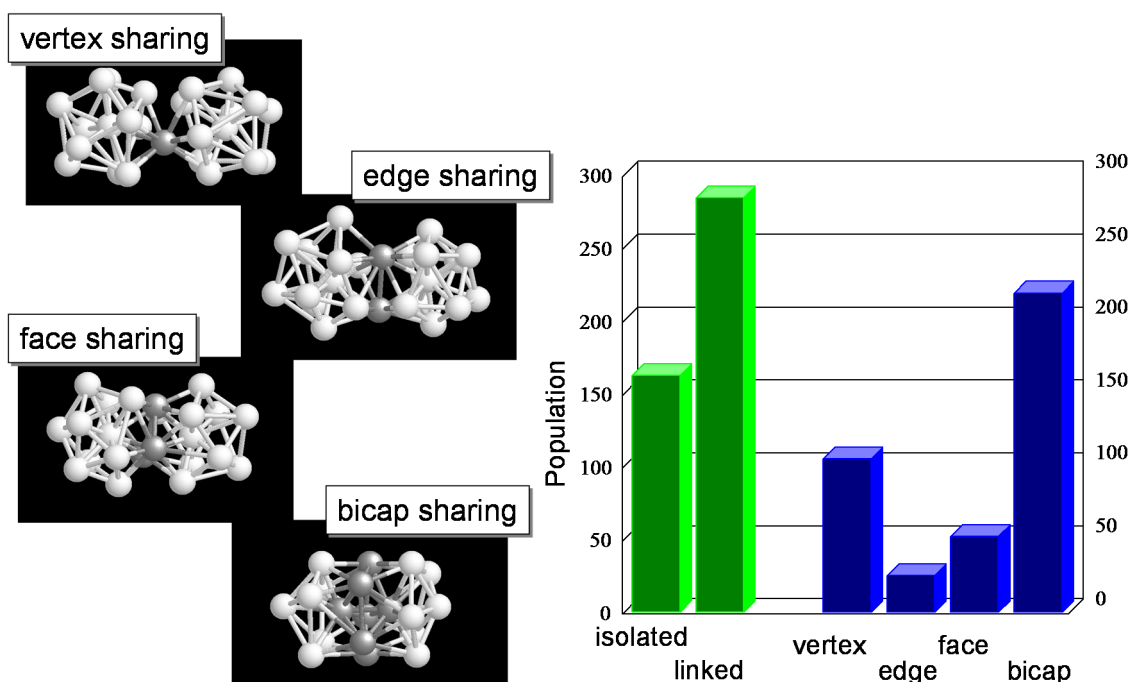


Figure 2. Linking patterns between the icosahedral clusters and their population found in an $N = 8000$ $Zr_{40}Cu_{60}$ glassy phase.

3.1.3. Icosahedral Order in Supercooled Liquids

The icosahedral clusters are also found in liquid phases. Figure 3 shows the temperature dependence of the atomic volume in a quenching process of the $N = 4000$ $Zr_{40}Cu_{60}$ system together with snapshots of icosahedral clusters found in supercooled liquid phases at $T = 1044$, 928 , and 814 K, where only the central atoms of the clusters are depicted by white spheres. In higher temperature liquid phases, most of the icosahedral clusters are isolated. As the temperature decreasing, a sign of networking can be found in supercooled liquid phases at near T_g .

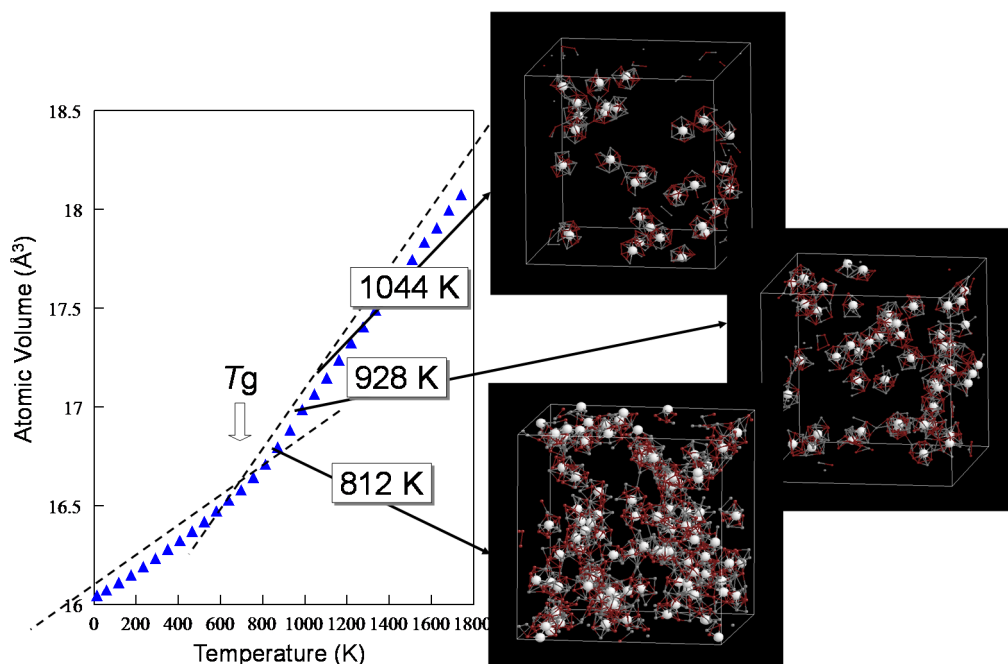


Figure 3. Volume change in a quenching process of the $N = 4000$ $Zr_{40}Cu_{60}$ alloy system and snapshots of icosahedral clusters formed in supercooled liquid phases, where the central atoms of the clusters are depicted by white spheres.

3.1.4. Lifetime of Icosahedral Clusters

The growth of the icosahedral order in supercooled liquid phases is closely related with the stability of the icosahedral clusters. To estimate it, we calculate the lifetime of the icosahedral clusters in supercooled liquids. The lifetime of the icosahedral cluster is defined as follows. Once an icosahedral cluster forms, the cluster is “living” when it keeps both the Voronoi index and the neighboring atoms. Let us show some illustrative examples. In Figure 4, the case (a) and the case (b) are considered to be “decaying” due to the change of symmetry or neighbors, but the case (c) is considered to be still “living” although the arrangement order of the neighbors are changed.

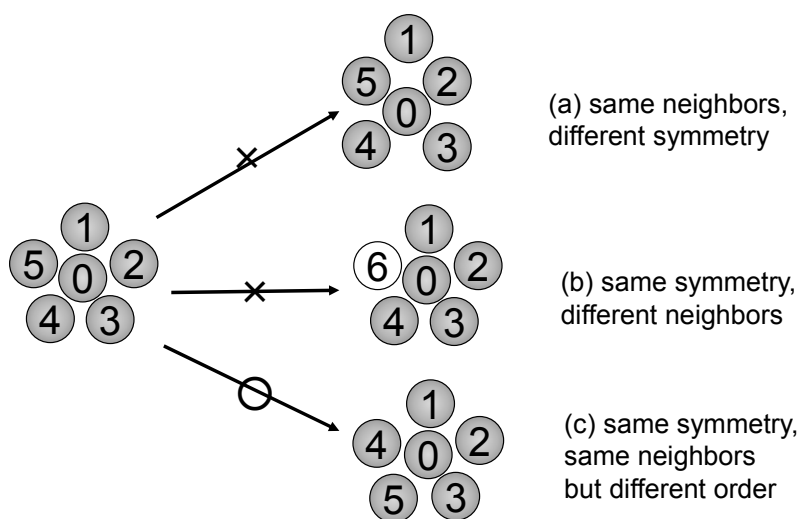


Figure 4. Changing patterns of atomic configuration of the cluster and definition of cluster decaying.

Under this definition, we have calculated the distribution of lifetime of the icosahedral clusters in supercooled liquid phases. Figure 5a shows the histogram of the lifetime of the clusters for 458 decaying events found in an $N = 4000$ $Zr_{40}Cu_{60}$ supercooled liquid phase at $T = 812$ K. More than 65% of the clusters has decayed within the first 2 ps after their formation, but the distribution of the lifetime has a long tail. Figure 5b shows the temperature dependence of the average lifetime in supercooled liquids of the $Zr_{40}Cu_{60}$ alloy system, where the average was taken from 458, 276, and 171 decaying events for the $T = 812$, 928, and 1044 K cases, respectively. The average lifetime goes longer at lower temperature and its temperature dependence indicates some activation process in the cluster decay. However, when we try to fit the lifetime distribution shown in Figure 5a to a single exponential function, we always failed at any temperature. Therefore, we try to fit the distributions by a stretched exponential function as $N(t) = N_0 \exp\{-(t/\tau)^\beta\}$. The results of the fitted values are $\beta = 0.74$ and $\tau = 0.72$ ps for $T = 812$ K. The fact that the exponent β is not unity indicates that the icosahedral cluster decaying cannot be described by a single process, and that there are two or more different processes with different time scales. Thus, we should investigate the time evolution of the decaying process of the icosahedral clusters more closely.

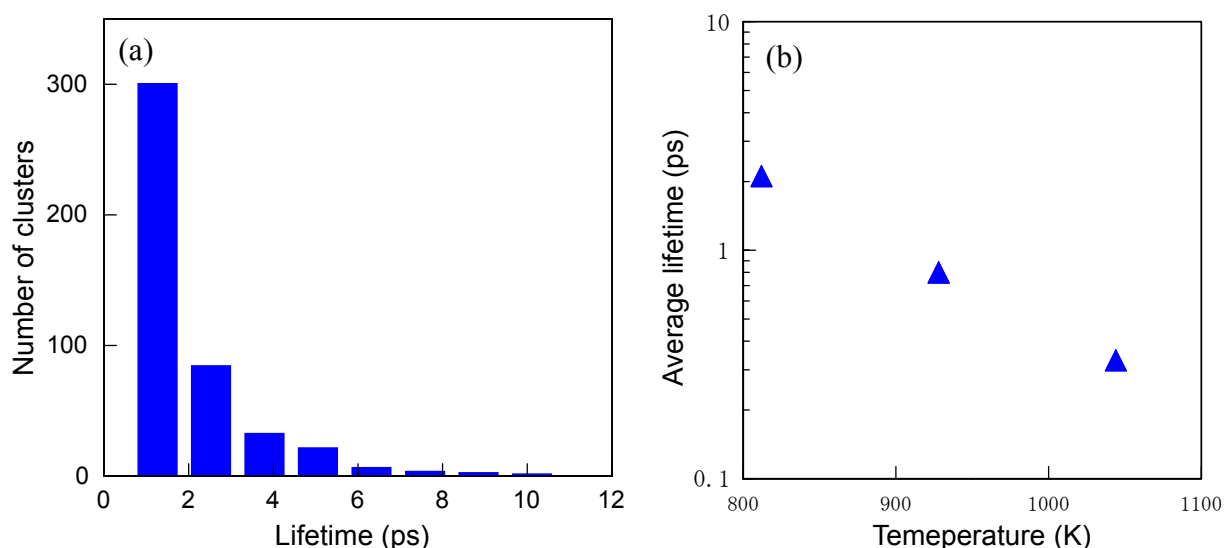


Figure 5. (a) Distribution of lifetime of the icosahedral clusters in an $N = 4000$ $Zr_{40}Cu_{60}$ supercooled liquid phase at $T = 812$ K and (b) temperature dependence of the average lifetime of the icosahedral clusters in liquid phases of the $Zr_{40}Cu_{60}$ alloy system.

3.1.5. Lifetime and Cluster Bonding

Let us show some examples of the cluster decaying process by depicting a series of snapshots of atomic configurations. Figure 6a is a snapshot of a supercooled liquid phase of the $N = 4000$ $Zr_{40}Cu_{60}$ system at just above T_g . More than 50 icosahedral clusters exist at this moment. Among them, we have picked up some clusters as shown in Figure 6b, where deep green atoms and deep red atoms denote isolated clusters, and light green ones and dark yellow ones denote connected clusters by bicap sharing. The colors of central atoms of the clusters are changed from those of their neighbors for eye guide, and the splitting of the dark yellow ones is due to the periodic boundary condition of the simulation cell. In the first frame at $t = 0$ (Figure 6b), all clusters keep the icosahedral symmetry. As the time goes on at $t = 0.5, 1.0, 1.5, 2.0$ ps (Figure 6c–f, respectively), the isolated clusters changed their neighbors and lost

their initial structure. On the other hand, the two-connected clusters (the light green atoms) and the three-connected clusters (the dark yellow atoms) keep their initial configurations even in the last frame at $t = 2.0$ ps (Figure 6f).

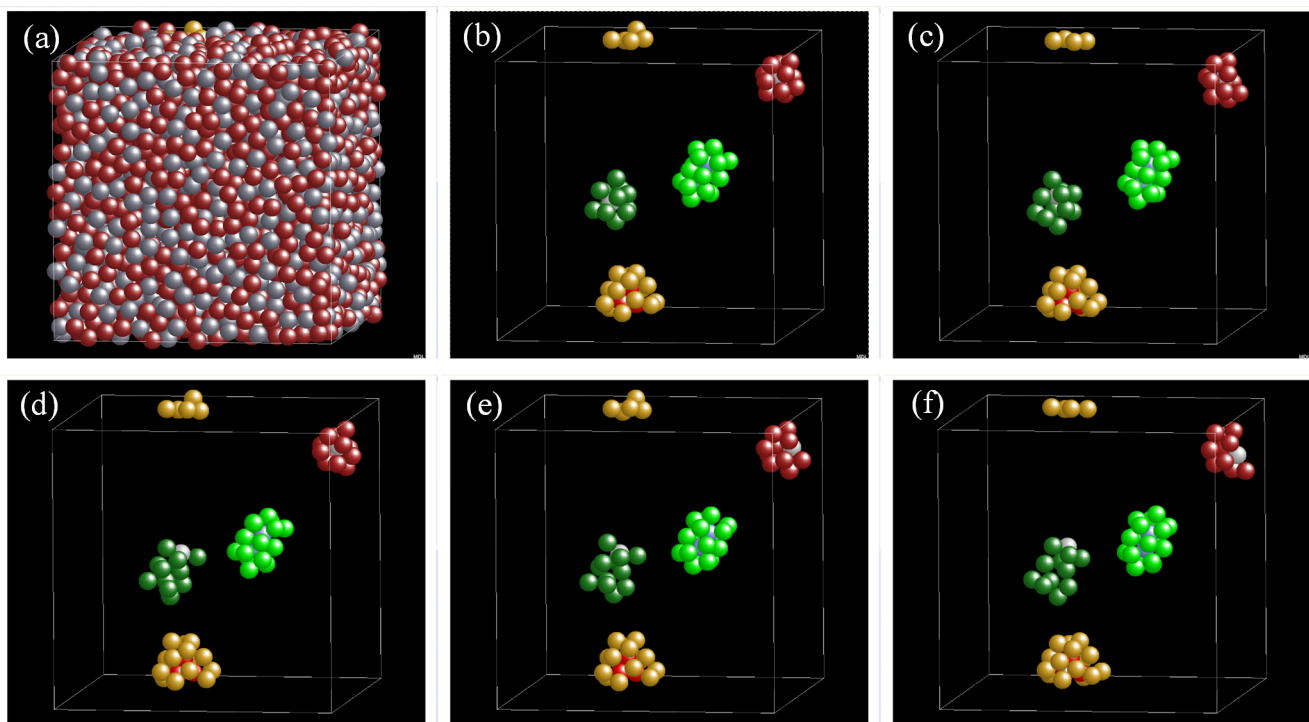


Figure 6. Snapshots of change of atomic configuration of icosahedral clusters in a supercooled liquid phase of the $Zr_{40}Cu_{60}$ system at just above T_g . (a) All atoms at $t=0$; (b) two isolated clusters and two connected “superclusters” picked up at $t = 0$; (c) configuration change at $t = 0.5$ ps; (d) at $t = 1.0$ ps; (e) at $t = 1.5$ ps; and (f) at $t = 2.0$ ps.

This behavior indicates that the cluster lifetime would be elongated by connecting to each other. Thus, we check the relation between lifetime and cluster networking. We calculated the average lifetime separately for isolated clusters, two-connected clusters, and multi-connected clusters with three or more connections in an $N = 4000$ $Zr_{40}Cu_{60}$ supercooled liquid phase at $T = 812$ K. The results are shown in Figure 7, where the average was taken from 30, 21, and 14 decaying events for the isolated, two-connected, and multi-connected clusters, respectively. We can see that the lifetime becomes longer if clusters are connected via bicap sharing, as already reported by Malins *et al.* [26] in a simulation study of a model binary glass former. Therefore, the icosahedral order in supercooled liquids is stabilized by the network formation of clusters connected via bicap sharing.

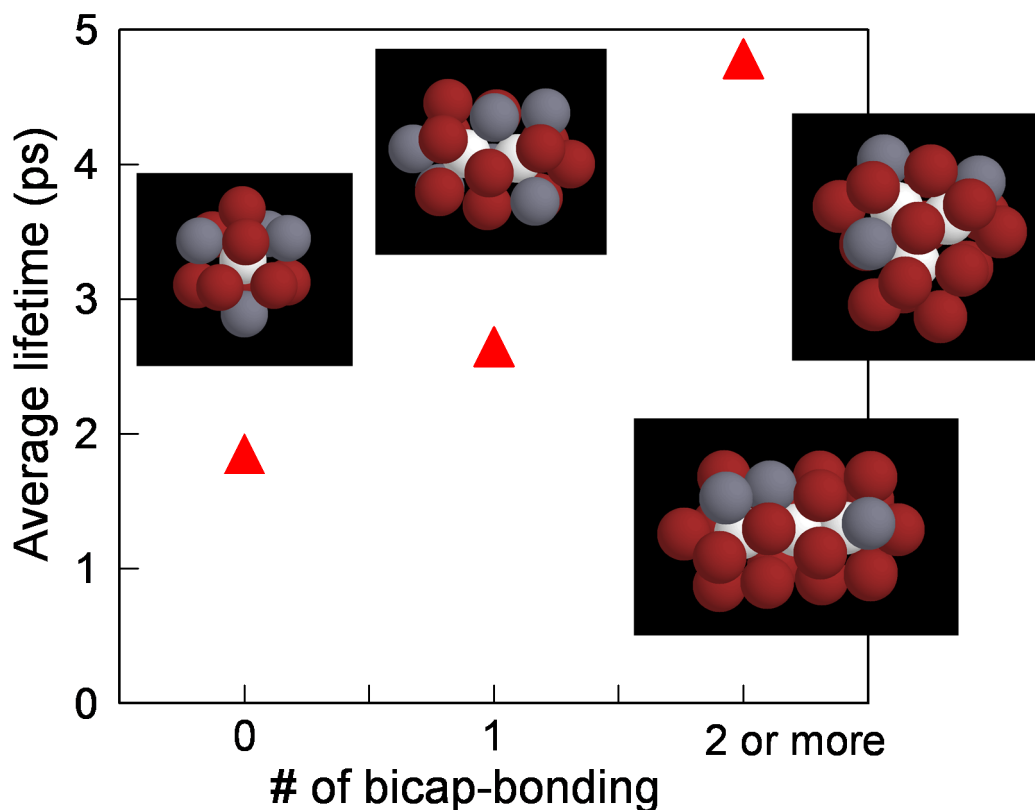


Figure 7. Relation between the average lifetime of the icosahedral clusters and the number of the bicap sharing bonds belonging to the clusters.

3.2. Icosahedral Order in Model System

3.2.1. Atomic Size Effect on Glass-forming Ranges of Model Binary System

To focus on a geometrical aspects of icosahedral order in metallic glasses, we proceed to analysis for a model alloy system interacting with the Lennard-Jones type potential, where we can freely change the atomic size ratio between constituent elements. Here we consider a model A-B binary alloy systems, where the element A has a unit size and the size of element B changes from 0.8 to 1, and the composition x_B of B is ranging from 0 to 1. The heat of mixing between the elements A and B is fixed to be zero to focus on a geometrical effect.

The glass-forming range by rapid quenching from liquid phases in this model system has been investigated in the previous studies [33–35] and the results are shown in Figure 8. The color of the glass-forming region indicates the cooling rate, where a darker region corresponds to a lower cooling rate. We can find that the glass-forming ability goes up as the atomic size difference increases.

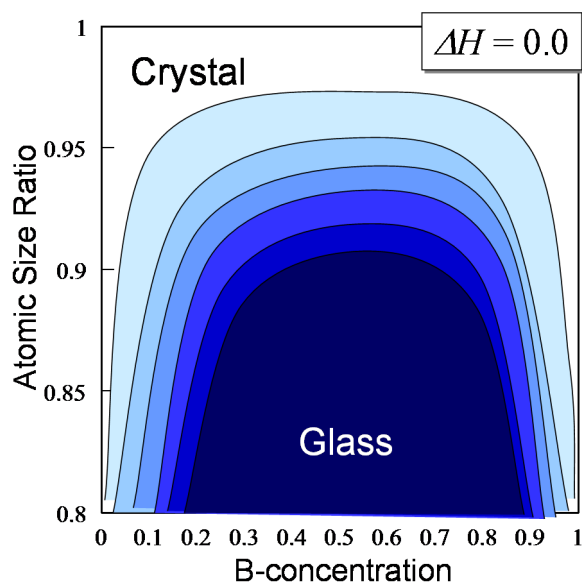


Figure 8. Dependence of glass-formation range on the cooling rate mapped on the atomic size ratio vs. composition plane. Darker region corresponds to lower cooling rate.

3.2.2. Geometrical Feature of Icosahedral Network

As found in the Zr-Cu system, we have found the network structure formed by icosahedral clusters mainly connected by bicap sharing in the glassy phases also in the model system. Figure 9 shows the properties of the cluster networks found in as-quenched glassy phases in the $N = 4000$ $A_{80}B_{20}$ and the $N = 4000$ $A_{40}B_{60}$ systems with the atomic size ratio 1:0.8, which approximately agrees with that between Zr and Cu atoms. The dominant connecting pattern is bicap sharing in both cases as found in the Zr-Cu system and the network is more extended in the $A_{40}B_{60}$ case than in the $A_{80}B_{20}$ case. If we pick up the cap sharing bonds and draw them as sticks, we can see that the network extends all over the system as shown in Figure 9b for the $A_{40}B_{60}$ case.

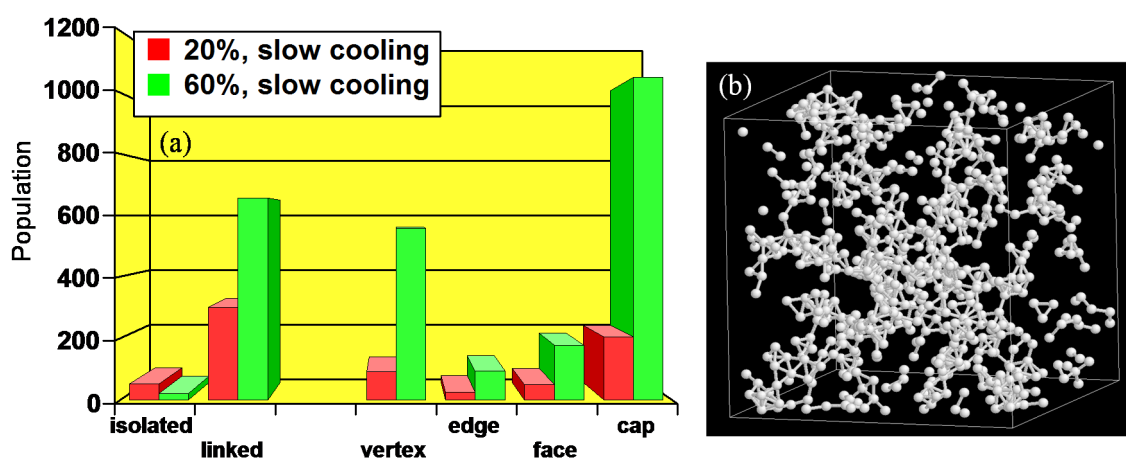


Figure 9. (a) Population of isolated/linked icosahedral clusters and those of linking patterns between clusters found in glassy phases of the $N = 4000$ $A_{80}B_{20}$ system and the $N = 4000$ $A_{40}B_{60}$ system; (b) Network structure formed by the bicap sharing bonds between the icosahedral clusters found in a glassy phase of the $A_{40}B_{60}$ system, where spheres and sticks denote the central atoms of the icosahedral clusters and the bicap sharing bonds, respectively.

3.2.3. Atomic Size Ratio Dependence of Icosahedral Order

The relation between the icosahedral order formation and the atomic size ratio is confirmed by investigating the icosahedral order in supercooled liquid phases. For a fixed composition $x_B = 0.5$, the dependence of the density of the icosahedral clusters on the atomic size ratio of the supercooled phases was calculated, and the results are shown in Figure 10. The number of icosahedral clusters in the supercooled liquids increases as the size difference increases to the atomic size ratio 1:0.8. On the other hand, it begins to decrease beyond the atomic size difference 0.2 because the relative stability of the icosahedral clusters to other types of clusters (e.g., the trigonal prisms [36]) decreases due to the large atomic size difference. It means that the proper size difference between constituent elements brings higher icosahedral order and higher stability of the supercooled liquid phases.

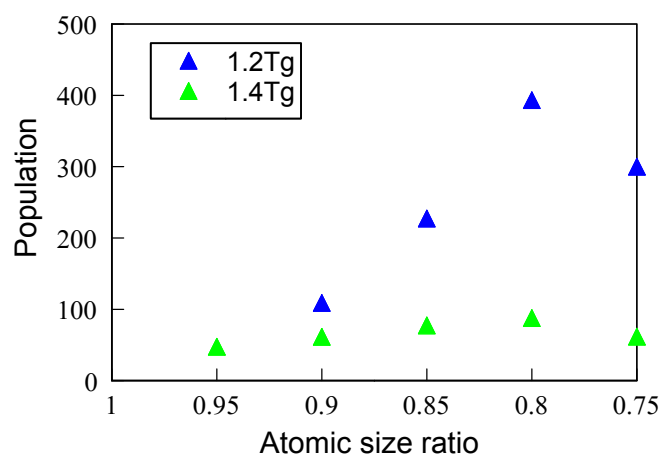


Figure 10. Dependence of the population of the icosahedral clusters in the supercooled liquid phases of the $N = 4000$ $A_{50}B_{50}$ system at $T = 1.4T_g$ and $T = 1.2T_g$ on the atomic size ratio.

3.2.4. Cluster Lifetime and Atomic Size difference

To estimate the stability of the icosahedral order in supercooled liquids in the model system, we have also calculated [35] the dependence of the average lifetime of the icosahedral clusters on the atomic size ratio. The results for supercooled liquids of the $N = 4000$ $A_{50}B_{50}$ system at $T = 1.2T_g$ are shown in Figure 11, where the average was taken from 45, 54, and 50 decaying events for the $A_{50}B_{50}$ system with the atomic size ratio 1:0.9, 1:0.85, and 1:0.8, respectively. The average lifetime of the clusters increases as the size difference increases in this range. The enhanced stability of the icosahedral clusters due to the atomic size difference would be mainly originated from two factors: One is enhancement of stability of single cluster due to atomic size difference and the other is enhancement of connectivity between the clusters due to the increase of cluster density. Since the stability of a sole cluster has been discussed in the previous study [35], we shall investigate the enhancement of the stability of the icosahedral order due to cluster connection by focusing on the geometry of cluster networking.

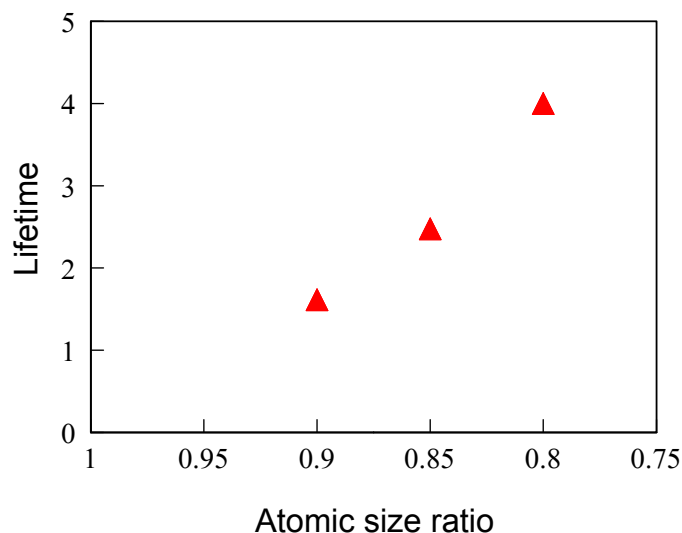


Figure 11. Dependence of the average lifetime of the icosahedral clusters in a supercooled liquid phase of the $N = 4000$ $A_{50}B_{50}$ system at $T = 1.2T_g$ on the atomic size ratio. The time unit normalized by the model parameters described in the Section 2.1 is used.

3.2.5. Icosahedral Network in Supercooled Liquids

The network structure of connected icosahedral clusters via bicap sharing is also observed in supercooled liquid phases. Figure 12 shows snapshots of the cluster networks found in supercooled liquid phases of the $N = 4000$ $A_{50}B_{50}$ system with the atomic size ratio 1:0.9 and 1:0.8, and the dependence of the number of cluster connection via bicap sharing in a supercooled liquid phase at $T = 1.2T_g$ on the atomic size ratio of the $N = 4000$ $A_{50}B_{50}$ system. Comparing with the cluster density shown in Figure 10, the number of bicap sharing bonds has larger dependence on the atomic size ratio. That is another reason why the stability of icosahedral structure in supercooled liquids is strongly enhanced by a large atomic size difference between alloying elements.

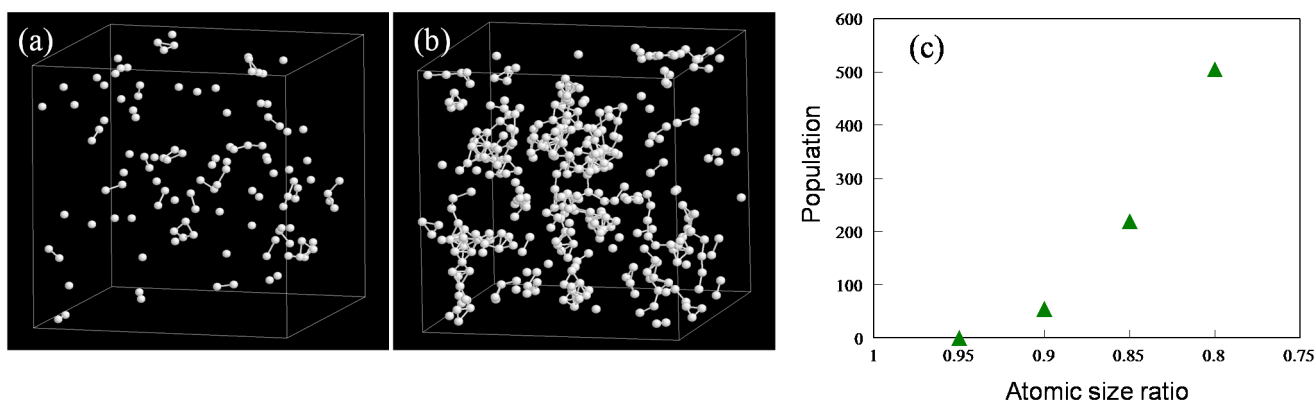


Figure 12. (a) Network structure formed by the bicap sharing bonds between the icosahedral clusters found in supercooled liquid phases of the $N = 4000$ $A_{50}B_{50}$ system with the atomic size ratio 1:0.9 and (b) the atomic size ratio 1:0.8, where spheres and sticks denote the central atoms of the icosahedral clusters and the bicap sharing bonds between clusters, respectively. (c) Dependence of the number of cluster connection via bicap sharing in a supercooled liquid phase of the $N = 4000$ $A_{50}B_{50}$ system at $T = 1.2T_g$ on the atomic size ratio.

3.2.6. Unit for 5-Fold Symmetry

The property of the network formed by bicap sharing bonds should depend on the properties of the sharing part of the bonding, that is, the pentagonal bicap formed by seven atoms. Therefore we shall change our focus from the icosahedral cluster to the pentagonal bicap or the bond surrounded by a 5-membered ring, which we call “5-ring bond”, as illustrated in Figure 13. Similarly we also call the bonds which are surrounded by 4 or 6 neighbors as 4-ring or 6-ring bonds, respectively.

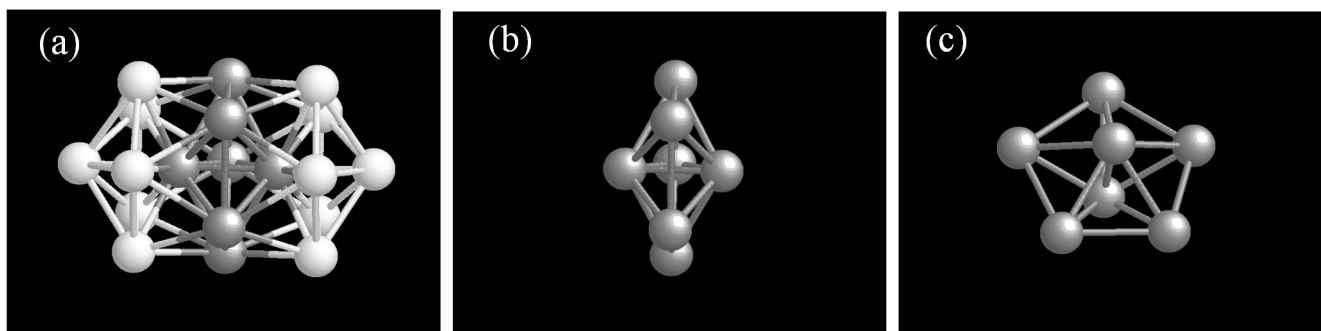


Figure 13. (a) Snapshot of two icosahedral clusters connected by bicap sharing; (b) Side view of a pentagonal bicap or a 5-ring bond formed by shared 7 atoms; and (c) perspective view of a 5-ring bond.

Here we add a note on the definition of “atomic bonding” in this study. We define that two atoms are “bonding” if the two atoms are sharing a common Voronoi face. This definition has the shortcomings that unnatural bonds might be generated when a large atomic size difference exists between constituent elements [37], because the atomic size is not taken into account in the Voronoi tessellation procedure. Therefore, one should use a kind of weighted Voronoi tessellation technique [37] for more detailed analyses.

3.2.7. Geometric Change in Solidification

To investigate the icosahedral order formation in solidifying stage, we calculate the temperature dependence of the population of 4-, 5- and 6-ring bonds together with that of icosahedral clusters in a quenching process of the $N = 4000$ $A_{50}B_{50}$ system with an atomic size ratio 1:0.8. The results are shown in Figure 14. The number of 5-ring bonds rapidly grows just above T_g as well as that of icosahedral clusters, which indicates that the icosahedral network by the bicap sharing connection would grow in this temperature range.

3.2.8. Geometric Change in Relaxation

We have also calculated the change of population of the 4-ring, 5-ring, and 6-ring bonds in a relaxation process of a glassy phase of the $A_{50}B_{50}$ system with the atomic size ratio 1:0.8 annealed just below T_g . The results are shown in Figure 15. We find that the 5-ring bonds increase and 4-ring bonds decrease in the relaxation stage. It indicates that the relaxation goes on with the growth of the 5-ring network supplied by transformation from 4-rings into 5-rings.

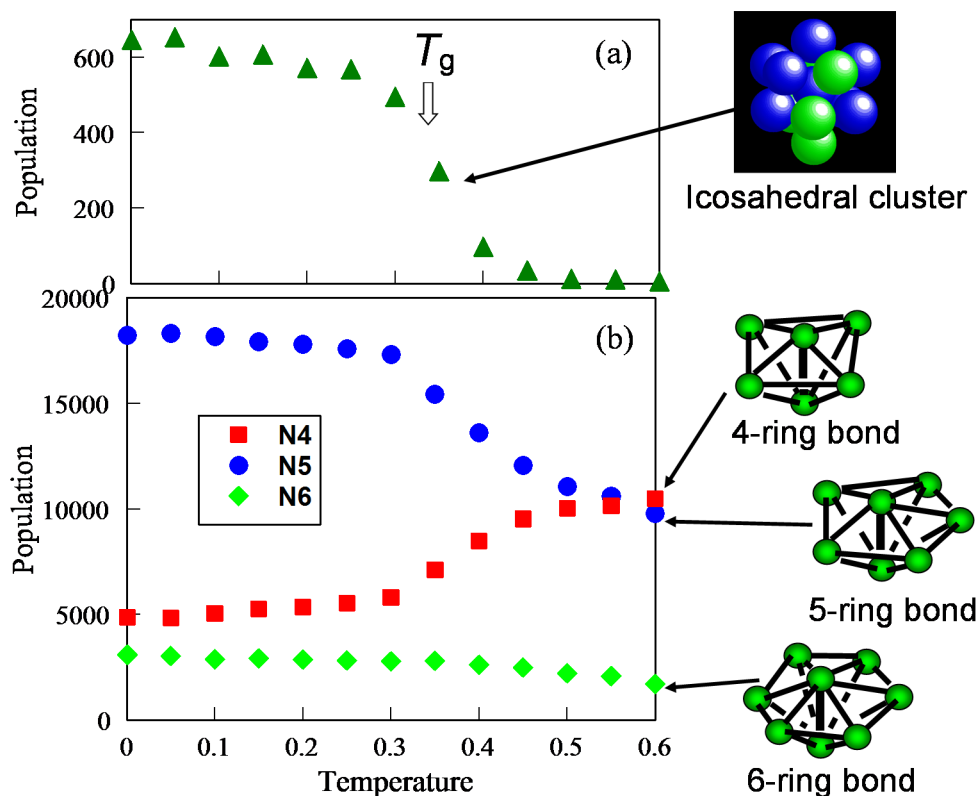


Figure 14. (a) Temperature dependence of population of the icosahedral clusters in a quenching process of the $N = 4000$ $A_{50}B_{50}$ system with an atomic size ratio 1:0.8; (b) Temperature dependence of population of the 4-ring, 5-ring, and 6-ring bonds in the same process.

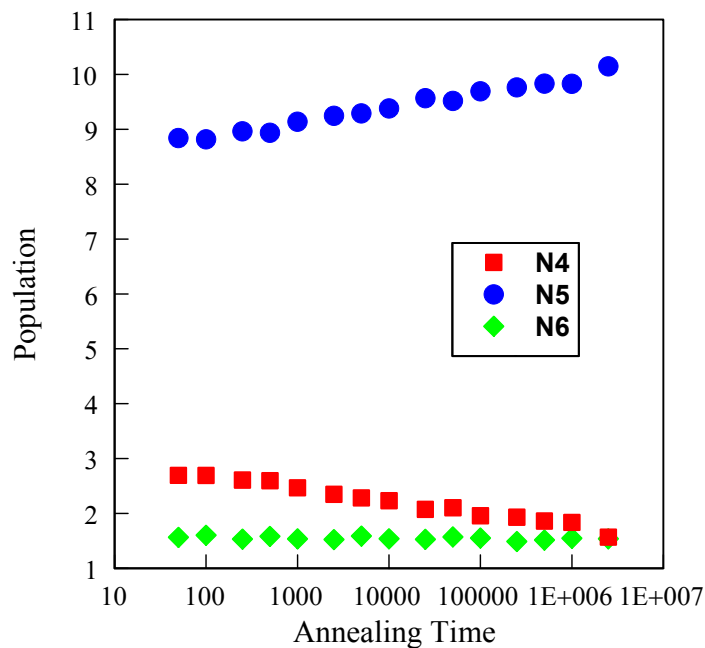


Figure 15. Time dependence of population of the 4-ring, 5-ring, and 6-ring bonds in an annealing process at just below T_g of the $N = 4000$ $A_{50}B_{50}$ system with an atomic size ratio 1:0.8.

3.3. Icosahedral Order and Regge Calculus

3.3.1. Geometric Consideration Based on DRP Model

The idea of the Dense Random Packing (DRP) [1] has given rise to various studies on the atomic structure of liquids and glasses [38–40]. The role of the 5-ring bond can be also understood by a simple geometric consideration based on the DRP model. In the DRP model, the basic building block is mutually bonded tetrahedral cluster of 4-atoms. In other words, the DRP structure is a space-filling with the tetrahedra in three dimensions. The fact that the regular tetrahedron has a dihedral angle around 70.5° , which cannot completely fit to 360° is the reason why the DRP structure cannot fill the whole three dimensional space as crystalline structures do. Therefore, the DRP structure is always accompanied with frustration. As illustrated in Figure 16, the 4-ring bond is too few, the 5-ring bond is a little few, and the 6-ring bond is too many. Among them, the 5-ring has the lowest frustration or distortion, which is why 5-rings dominate in DRP structure.

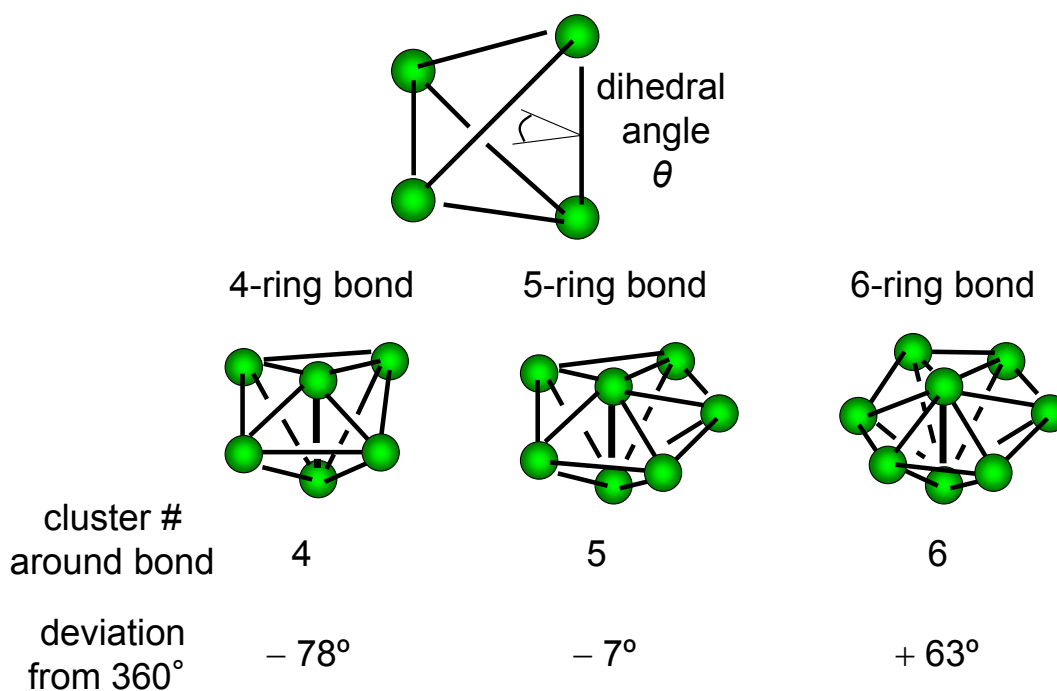


Figure 16. Tetrahedral cluster and 4-, 5-, and 6-ring bonds and the deficit angles around each bonds.

3.3.2. Regge Calculus

To estimate this type of distortion energy, the Regge calculus [41,42] is an appropriate formalism, which was originally proposed as a model of theory of gravitation. In Einstein's theory of gravity, the energy of continuum space-time is expressed by a scalar curvature. On the other hand, in the Regge calculus, the space-time is discretized into simplices (*i.e.*, triangles in two dimensions and tetrahedra in three dimensions) and the energy is estimated by the deviation from 360° or the “deficit angle” located at “hinge”. As illustrated in Figure 17, the deficit angle is located at each vertex in two dimensions.

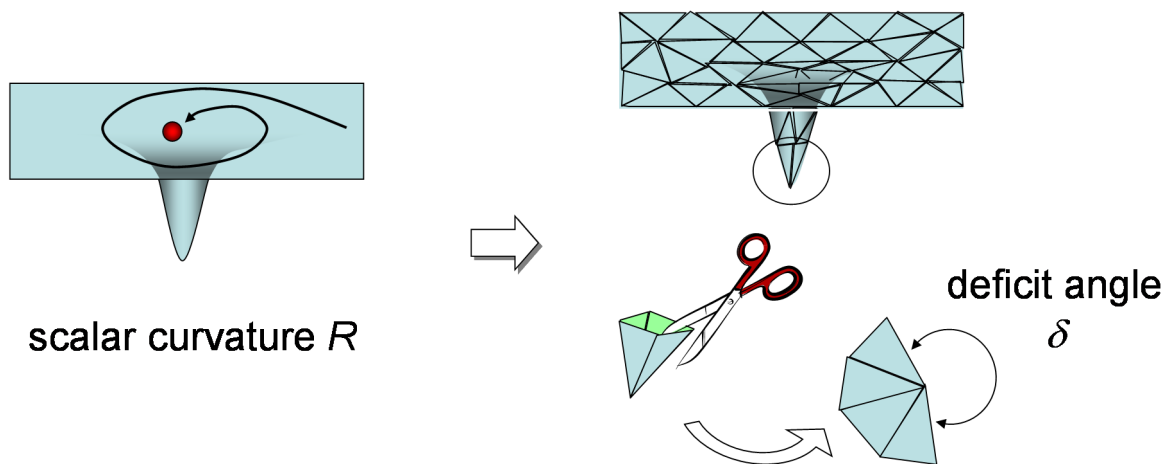


Figure 17. Illustrative view between the continuum theory and the discrete theory of curvature in two-dimensional manifold.

In three dimensions, the space is divided by tetrahedra, and the deficit angle is located at each link or bond, as illustrated in Figure 18. Thus, the hinges are vertices in two dimensions and links in three dimensions.

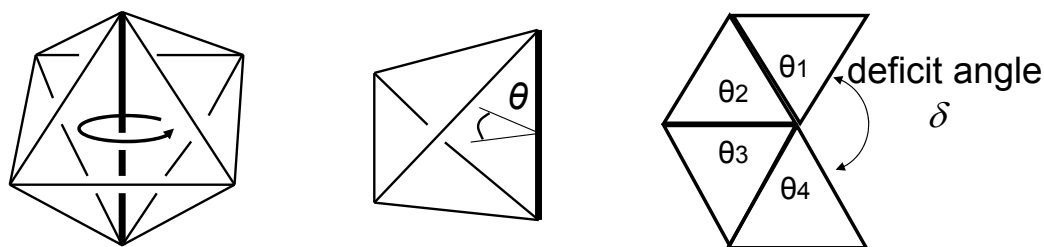


Figure 18. Illustrative view of definition of deficit angle around a bond in three dimensions.

3.3.3. Variety of Tetrahedral Building Blocks: Binary Case

For a monoatomic system, there is no variation of shape of tetrahedra but the regular tetrahedron, so the lowest energy bond for pure elements is the 5-ring bond. On the other hand, if we introduce the different sized elements, the shape variation of tetrahedra increases and the variation of dihedral angles also goes up, as illustrated in Figure 19 for a binary AB system with an atomic size ratio 1:0.8.

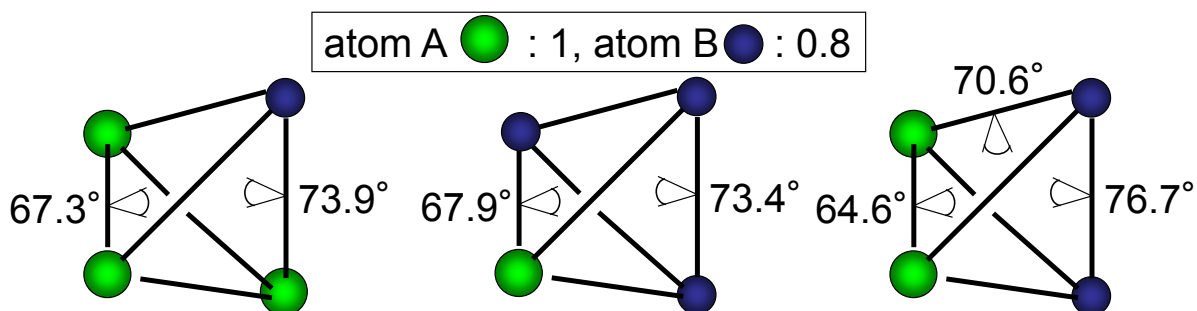


Figure 19. Variety of dihedral angles of tetragonal clusters found in a binary system with the atomic size ratio 1:0.8.

In this binary system, we have 24 different configurations of 5-rings. Among them we can find six configurations which has a lower distortion or a smaller deficit angle than that of monoatomic 5-rings as shown in Figure 20. These configurations of 5-rings with lower distortion would be the key structure to construct an icosahedral ordered network with low frustration in the alloy system.

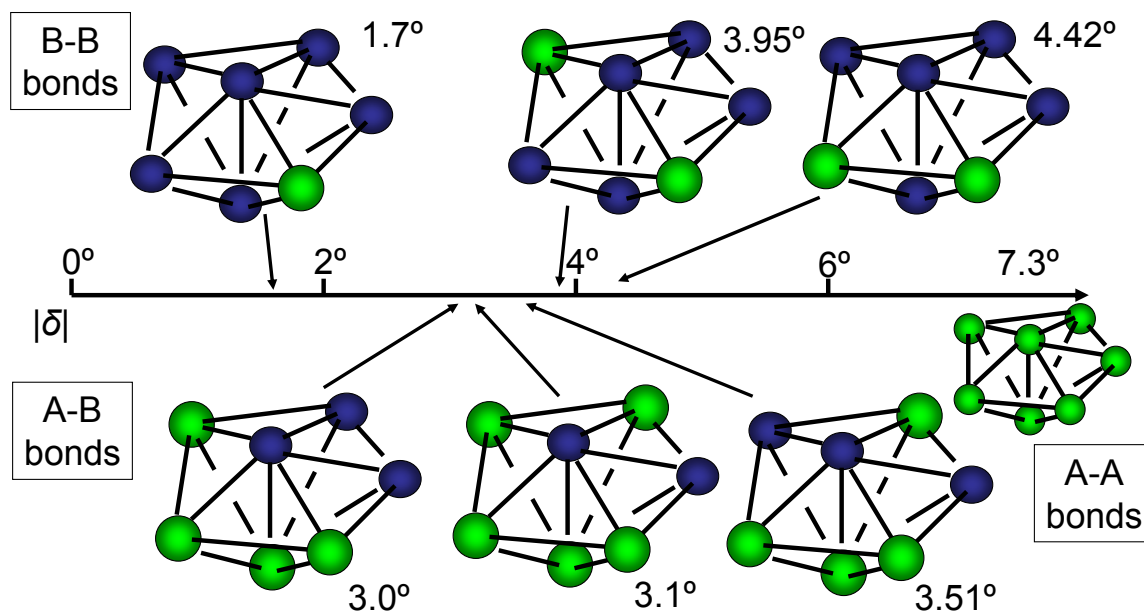


Figure 20. Configurations of 5-ring bonds which has a smaller deficit angle found in a binary system with the atomic size ratio 1:0.8 than that of the 5-ring bond in monoatomic systems.

3.3.4. Icosahedral Network and Low Distortion 5-Rings

The frustration in the network formed by bicap sharing bonds would get lower and the connectivity of the network would be enhanced by the existence of these types of low distortion 5-rings. Therefore, we examined the distribution and population of these types of 5-rings in the icosahedral network via bicap sharing in glassy phases of the AB system. Figure 21 shows snapshots of the icosahedral networks formed by bicap sharing bonds and their portions consisting the top 6 types of low distortion 5-rings shown in Figure 20 found in an as-quenched glassy phase of the $N = 4000$ $A_{50}B_{50}$ system with the atomic size ratio 1:0.8. The top 6 configurations of 5-rings distribute over all icosahedral networks of bicap sharing and its fraction in the network is 50.9%, which is considerably greater than the expectation value $45/128 = 35.2\%$ of finding the above six configurations when we make 5-rings by randomly choosing seven atoms from A or B atoms with equal probability from the $A_{50}B_{50}$ composition. Figure 21c,d shows a bonding topology and the atomic configuration of a portion of the icosahedral network connecting solely the top six configurations of 5-rings.

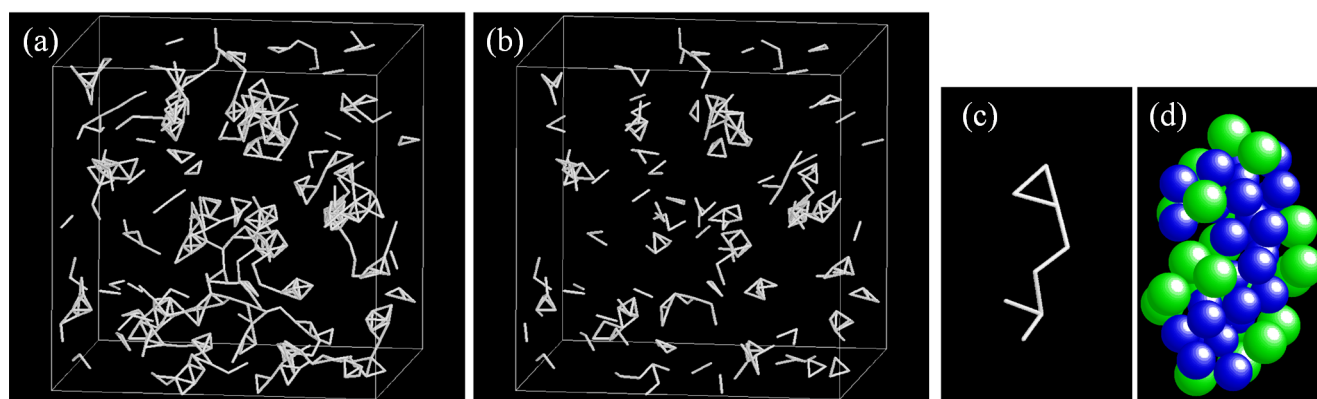


Figure 21. (a) Snapshot of the icosahedral networks linked by bicap sharing and (b) their portions consisting of the top six configurations with low distortion as depicted in Figure 20 found in an as-quenched glassy phase of the $N = 4000$ $A_{50}B_{50}$ system with the atomic size ratio 1:0.8. (c) Snapshot of bonding topology of a fragment of the network shown (b), and (d) atomic configuration of this portion formed by eight icosahedral clusters, where green and blue spheres denote the A and B atoms, respectively.

3.3.5. Geometry Change in Relaxation

The top six configurations with lower distortion of 5-ring bonds are already dominated in the as-quenched glassy phases as expected. It is likely that their fraction in the icosahedral network would grow in the course of structural relaxation. The results are shown in Figure 22 for an annealing process at just below T_g of a glassy phase of the $N = 4000$ $A_{50}B_{50}$ system with an atomic size ratio 1:0.8. The population of these top six configurations has grown in the annealing process, as well as the total number of bicap 5-ring bonds. However, the fraction of them little changed and simply fluctuated within $50\% \pm 3\%$ during the annealing process. It means that the relaxation goes mainly by 5-rings formation supplied by 4-rings decay into 5-rings as found in Figure 15, and that the contribution from the configuration change in 5-rings is small, due to low mobility in glassy phases. In other words, the average alloy composition is important to form a lower distortion network of the icosahedral clusters.

3.3.6. Low Distortion 5-Rings and Alloy Compositions of Good Glass-Former

From that viewpoint, we discuss the relation between the composition dependence of icosahedral order and the atomic configurations of 5-rings for the model binary system with the atomic size ratio 1:0.8. As an index for the icosahedral order formation, we calculate the number of the bicap sharing bonds in the networks of icosahedral clusters formed in supercooled liquid phases at $T = 1.2T_g$ of the $N = 4000$ AB system with the atomic size ratio 1:0.8. The results are shown in Figure 23. In this viewgraph, we have indicated the average composition of the 5-rings which have lower distortion as illustrated in Figure 20. Based on the composition dependence of icosahedral order, the predicted composition of the highest icosahedral order and the best glass-former is around $x_B = 0.60$. On the other hand, the composition of the 5-ring of the lowest distortion and the average composition of top 6 configurations are 0.86 and 0.57, respectively, the latter of which is not so bad prediction for highest

icosahedral order and good glass-former. It means that the alloy composition which has the biggest chance to form the low distortion 5-rings would be a good glass-former.

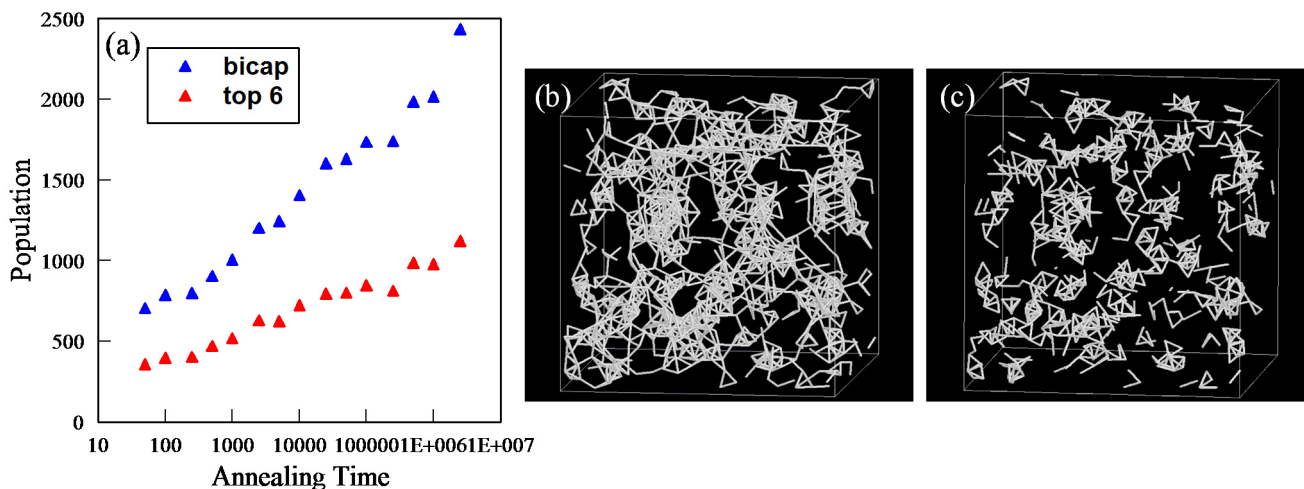


Figure 22. (a) Time evolution of the number of the bicap sharing bonds between icosahedral clusters and that of the top 6 configurations of 5-rings in the bicap connections in an annealing process at just below T_g of a glassy phase of the $N = 4000$ $A_{50}B_{50}$ system with an atomic size ratio 1:0.8; (b) Snapshot of the icosahedral network via bicap sharing formed in a relaxed glassy phase (annealing time: 2.5×10^6); and (c) portion of the top six configurations in the icosahedral network.

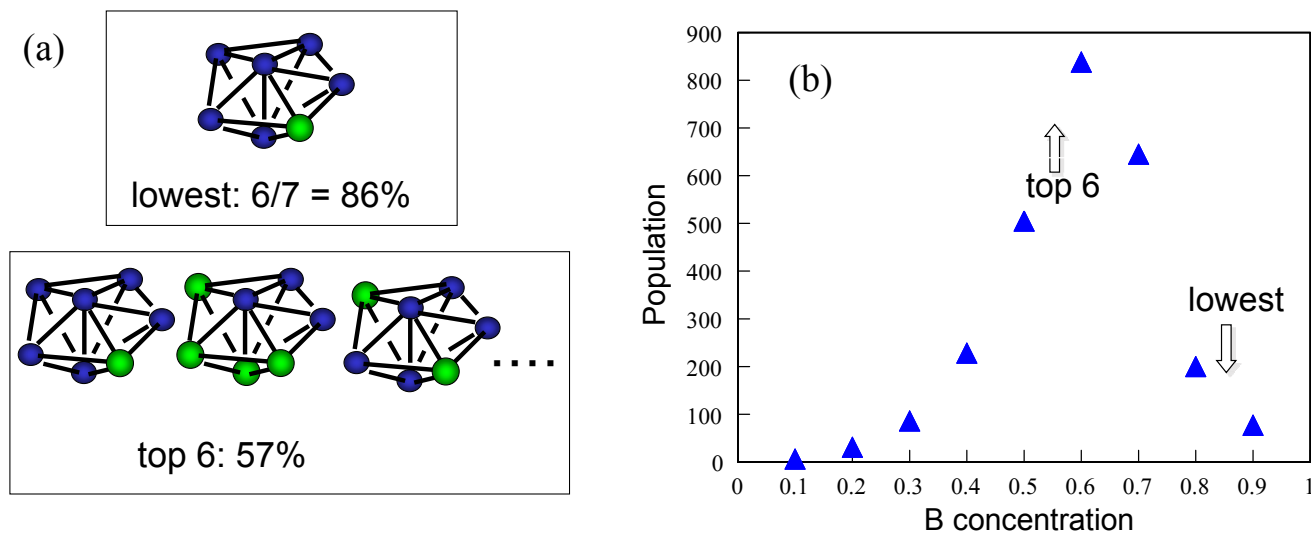


Figure 23. Comparison between the alloy composition of clusters with lower distortion and that of higher density of icosahedral order. (a) Atomic configuration of 5-ring bonds with lower distortion; (b) Composition dependence of the number of the bicap sharing bonds between the icosahedral clusters in supercooled liquid phases at $T = 1.2T_g$ of the $N = 4000$ AB system with the atomic size ratio 1:0.8. The arrows indicate the composition of the clusters shown in Figure 23a.

3.3.7. Variety of Tetrahedral Building Blocks: Ternary Case

For ternary system with size ratio 1:0.9:0.8, we have further variety of tetrahedron shape. Consequently, we can find many lower distortion configurations in the ternary system than those in binary systems, as shown in Figure 24. That is why the glass-forming ability goes up in ternary or more components metallic systems.

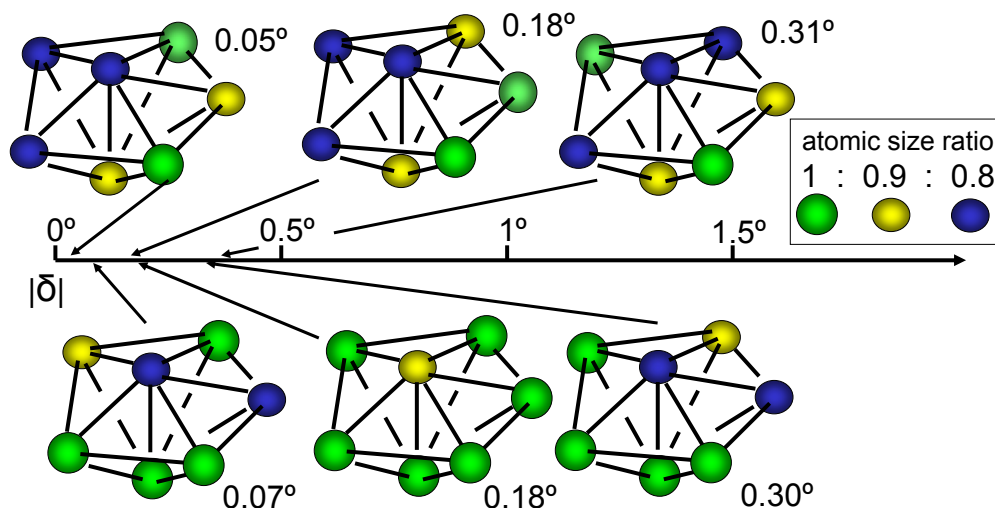


Figure 24. Configurations of 5-ring bonds which have a smaller deficit angle than 0.5 degree found in a ternary system with the atomic size ratio 1:0.9:0.8.

The well-known three empirical rules to acquire a high glass-forming ability in metallic systems proposed by Inoue [31] are the following:

- (1) Multicomponent alloy systems consisting of more than three components,
- (2) Significantly different atomic size ratios among the main constituent elements,
- (3) Large negative heats of mixing among their elements.

The first one (multi-component) and the second one (large atomic size difference) would realize the 5-ring configurations with very low distortion just as shown in Figure 24. Moreover, the third one (negative heat of mixing) makes the probability of forming such low distortion 5-rings greater, because such configurations can be achieved only by mixing different components as shown in Figure 24. In this sense, we can understand the above rules as criteria for lower distortion network formation of icosahedral order.

From a similar point of view, we can understand the geometrical origin of medium-range order structure in metallic glasses by constructing a structural model of icosahedral order by connecting lower strain 5-rings step by step. In the course of construction, we should take not only the icosahedral clusters but also the distorted icosahedra, which are not indexed (0, 0, 12, 0), into account. This type of construction would offer a geometrical basis of the “low frustrated disclination line” [42] or the “icosahedral backbone” [18,19]. This task is complicated and will be the subject of further studies.

3.3.8. Relation between Icosahedral Clusters and Other Types of Clusters

As a structural unit, not only the icosahedral clusters indexed as (0 0 12 0) but other types of clusters also play an important role in liquid and glassy phases of metallic glasses. Lee *et al.* has shown [19] in their simulation study that the interconnection between the icosahedral network and distorted icosahedra (for example, indexed as (0 2 8 2)) form a medium-range structure in the Cu-Zr glassy phases. Ding *et al.* has shown [22] that icosahedral clusters are only dominated in the Cu-centered clusters, but another type of Frank-Kasper polyhedra indexed as (0 0 12 4) called “Z16 cluster” are dominated in the Zr-centered clusters and both types of clusters contribute to the icosahedral order formation in the Cu-Zr supercooled liquids. It means that the icosahedral cluster are only important around “smaller” atoms, but other type of clusters is important around “larger” atoms. Here we should note that the central atom of the Z16 cluster has twelve 5-ring bonds and four 6-ring bonds, so an increase of the Z16 clusters may also contribute to the formation of icosahedral order or 5-ring networks as in the case of the icosahedral clusters. In addition, recent experimental observations [24] and simulation studies [26] have shown that the crystal-like clusters also play an important role in the dynamics at the glass transition, where the time scale of structural relaxation blows up. Therefore, we discuss the interrelation between the icosahedral clusters and other types of clusters for the model binary system shortly.

For the $N = 4000$ A₅₀B₅₀ system with an atomic size ratio 1:0.8, the fraction of Voronoi polyhedra with various indices was calculated for an as quenched glassy phase and an relaxed glassy phase annealed at just below T_g for $\Delta t = 2.5 \times 10^6$. The results are shown in Figure 25a, where some of the most abundant polyhedra are shown in each symmetry, that is, the icosahedron-like, the Z16 cluster-like, and crystal-like symmetry. In both cases, the most populous polyhedron is the icosahedron and the next one is the distorted icosahedron indexed by (0 1 10 2). In the relaxed glassy phase, the fraction of the icosahedron-like atoms and Z16 cluster-like atoms have increased due to the structural relaxation. Among them, the fraction of the Z16 cluster showed a remarkable growth (2.75 times higher) [22]. On the other hand, the fraction of crystal-like atoms has a little decreased and it indicates that the crystal-like clusters would transform into the icosahedral ones by annealing, which is consistent with a recent experimental observation in Zr₅₀Cu₄₅Al₅ bulk metallic glasses [11]. In the same relaxed phase, 96.7% of the icosahedron-like clusters are the (smaller) B atom-centered, while 99.7% of the Z16 cluster-like clusters are the (larger) A atom-centered.

To get a hint of the structural roles of various types of clusters, we have shown a snapshot of spatial distribution of them in Figure 25b, where a 25% portion of the $N = 4000$ relaxed glassy A₅₀B₅₀ alloys is sliced out and only the atoms centered at the icosahedral clusters, the distorted icosahedra, the Z16 cluster, the Z16 cluster-like ones, and the crystal-like ones are depicted by the white, yellow, dark green, light green, and blue spheres. From the figure, the distorted icosahedral atoms and the Z16 cluster-like atoms seem to interconnect to the icosahedral network and form a larger network structure, while the crystal-like atoms seem to occupy a little separated region from the icosahedral network. Clarifying the individual roles of the icosahedral, the distorted icosahedral, and Z16 cluster-like atoms in forming the icosahedral medium-range order is an important issue to be investigated but will be another subject of our future studies.

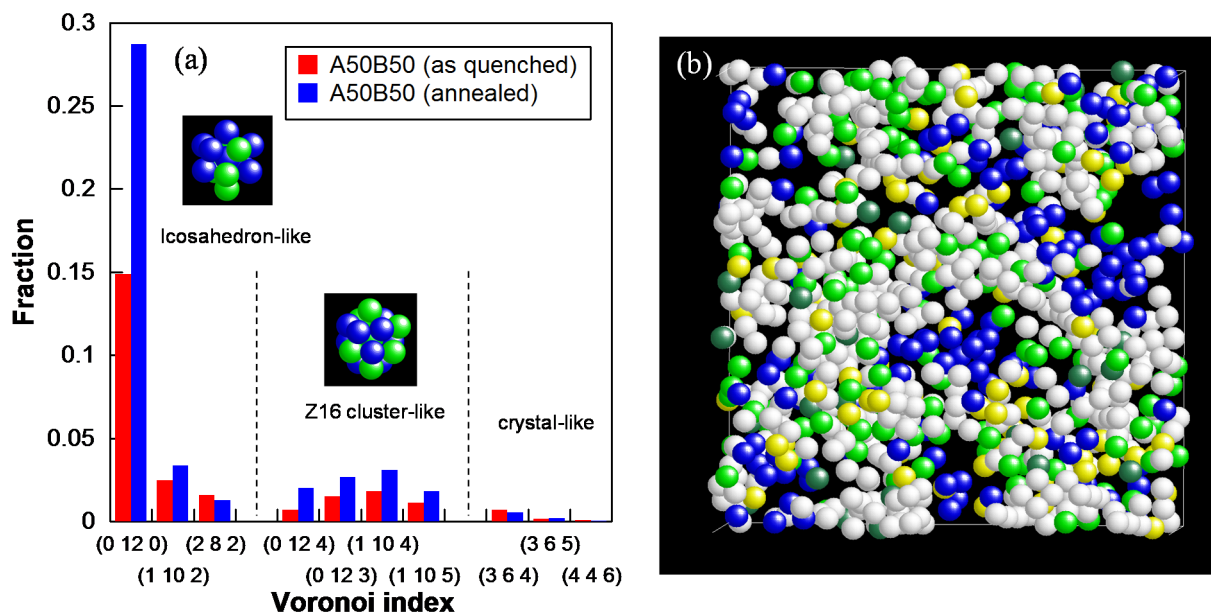


Figure 25. (a) Fractions of various Voronoi polyhedra found in an as quenched glassy phase (**green**) and a relaxed glassy phase (**blue**) of the $N = 4000$ $A_{50}B_{50}$ system with an atomic size ratio 1:0.8; (b) Snapshot of atomic configuration of a 25% portion of an $N = 4000$ relaxed glassy $A_{50}B_{50}$ phase. Only the atoms centered at the icosahedral clusters, the distorted icosahedra, the Z16 clusters, the Z16 cluster-like ones, and the crystal-like ones are depicted by the white, yellow, dark green, light green, and blue spheres.

4. Conclusions

Icosahedral ordered structures formed in liquid and glassy phases of metallic glasses are investigated by using molecular dynamics simulations. In both the Zr-Cu alloy system and a model binary alloy systems, the same feature of the icosahedral order is observed. Formation and decay processes of the icosahedral clusters are found in liquid phases. As the temperature decreases, the lifetime of the cluster becomes longer and the density of the cluster grows in supercooled liquid phases. Near T_g , the clusters begin to connect to each other and the network structure of clusters connected via bicap sharing forms, which is the origin of the icosahedral medium-range order. Network formation of icosahedral clusters via cap-sharing in supercooled liquids enhances stability of clusters. In glassy phases, the icosahedral network grows and extends over the whole system in structural relaxation by annealing. The frustration or distortion in the icosahedral network formed by bicap or 5-ring sharing connections can be estimated by using the Regge calculus. The analysis of the distortion in the connected part or the 5-ring bond shows that atomic size difference gives a variety in shape of tetrahedral clusters and generates lower frustrated configurations of 5-ring bonds and icosahedral clusters. The empirical rules between alloying elements for achieving high glass-forming ability in metallic systems can be understood by the analysis of the frustration of the 5-rings.

Author Contributions

The authors contributed equally to this work.

Conflicts of Interest

The authors declare no conflict of interest.

References

1. Bernal, J.D. A Geometrical Approach to the Structure of Liquids. *Nature* **1959**, *183*, 141–147.
2. Cargill, G.S., III. Dense random packing of hard spheres as a structural model for noncrystalline metallic solids. *J. Appl. Phys.* **1970**, *41*, 2248–2250.
3. Finney, J.L. Modelling the structures of amorphous metals and alloys. *Nature* **1977**, *266*, 309–314.
4. Yamamoto, R.; Doyama, M. The polyhedron and cavity analyses of a structural model of amorphous iron. *J. Phys. F Metal Phys.* **1979**, *9*, 617–627.
5. Inoue, A.; Zhang, T.; Masumoto, T. Zr-Al-Ni amorphous alloys with high glass transition temperature and significant supercooled liquid region. *Mater. Trans. JIM* **1990**, *31*, 177–183.
6. Parker, A.; Johnson, W.L. A highly processable metallic glass: $Zr_{41.2}Ti_{13.8}Cu_{12.5}Ni_{10}Be_{22.5}$. *Appl. Phys. Lett.* **1993**, *63*, 2342–2344.
7. Saida, J.; Sanada, T.; Sato, S.; Imafuku, M.; Matsubara, E.; Inoue, A. Local structure study in Zr-based metallic glasses. *Mater. Trans.* **2007**, *48*, 1703–1707.
8. Hui, X.; Gao, R.; Chen, G.L.; Shang, S.L.; Wang, Y.; Liu, Z.K. Short-to-medium-range order in $Mg_{65}Cu_{25}Y_{10}$ metallic glass. *Phys. Lett. A* **2008**, *372*, 3078–3084.
9. Shen, Y.T.; Kim T.H.; Gangopadhy, A.K.; Kelton, K.F. Icosahedral order, frustration, and the glass transition: Evidence from time-dependent nucleation and supercooled liquid structure studies. *Phys. Rev. Lett.* **2009**, *102*, 057801.
10. Hirata, A.; Guan, P.-F.; Fujita, T.; Hirotsu, Y.; Inoue, A.; Yavari, A.R.; Sakurai, T.; Chen, M.-W. Direct observation of local atomic order in a metallic glass. *Nat. Mater.* **2011**, *10*, 28–32.
11. Hwang, J.; Melgarejo, Z.H.; Kalay, Y.E.; Kalay, I.; Kramer, M.J.; Stone, D.S.; Voyles, P.M. Nanoscale Structure and Structural Relaxation in $Zr_{50}Cu_{45}Al_5$ Bulk Metallic Glass. *Phys. Rev. Lett.* **2012**, *108*, 195505.
12. Liu, A.C.Y.; Neish, M.J.; Stokol, G.; Buckley, G.A.; Smillie, L.A.; de Jonge, M.D.; Ott, R.T.; Kramer, M.J.; Bourgeois, L.J. Systematic Mapping of Icosahedral Short-Range Order in a Melt-Spun $Zr_{36}Cu_{64}$ Metallic Glass. *Phys. Rev. Lett.* **2013**, *110*, 205505.
13. Miracle, D.B. A structural model for metallic glasses. *Nat. Mater.* **2004**, *3*, 697–702.
14. Sheng, H.W.; Luo, W.K.; Alamgir, F.M.; Bai, J.M.; Ma, E. Atomic packing and short-to-medium-range order in metallic glasses. *Nature* **2006**, *439*, 419–425.
15. Shimono, M.; Onodera, H. Icosahedral order in supercooled liquids and glassy alloys. *Mat. Sci. Forum* **2007**, *539–543*, 2031–2035.
16. Wakeda, M.; Shibutani, Y. Icosahedral clustering with medium-range order and local elastic properties of amorphous metals. *Acta Mater.* **2010**, *58*, 3963–3969.
17. Xie, Z.-C.; Gao, T.-H.; Guo, X.-T.; Qin, X.-M.; Xie, Q. Growth of icosahedral mediumrange order in liquid TiAl alloy during rapid solidification. *J. Non-Cryst. Solids* **2014**, *394*, 16–21.
18. Li, M.Z.; Wang, C.Z.; Hao, S.G.; Kramer, M.J.; Ho, K.M. Structural heterogeneity and medium-range order in Zr_xCu_{100-x} metallic glasses. *Phys. Rev. B* **2009**, *80*, 184201.

19. Lee, M.; Kim, H.-K.; Lee, J.-C. Icosahedral medium-range orders and backbone formation in an amorphous alloy. *Met. Mater. Int.* **2010**, *16*, 877–881.
20. Cheng, Y.Q.; Ma, E.; Sheng, H.W. Atomic level structure in multicomponent bulk metallic glass. *Phys. Rev. Lett.* **2009**, *102*, 245501.
21. Lekka, Ch.E.; Evangelakis, G.A. Bonding characteristics and strengthening of CuZr fundamental clusters upon small Al additions from density functional theory calculations. *Scr. Mater.* **2009**, *61*, 974–977.
22. Ding, J.; Cheng, Y.-Q.; Ma, E. Full icosahedra dominate local order in Cu₆₄Zr₃₄ metallic glass and supercooled liquid. *Acta Mater.* **2014**, *69*, 343–354.
23. Frank, F.C.; Kasper, J.S. Complex alloy structures regarded as sphere packings. I. Definitions and basic principles. *Acta Cryst.* **1958**, *11*, 184–190.
24. Leocmach, M.; Tanaka, H. Roles of icosahedral and crystal-like order in the hard spheres glass transition. *Nat. Commun.* **2012**, *3*, 974.
25. Pedersen, U.R.; Schröder, T.B.; Dyre, J.C.; Harrowell, P. Geometry of Slow Structural Fluctuations in a Supercooled Binary Alloy. *Phys. Rev. Lett.* **2010**, *104*, 105701.
26. Malins, A.; Eggers, J.; Royall, C.P.; Williams, S.R.; Tanaka, H. Identification of long-lived clusters and their link to slow dynamics in a model glass former. *J. Chem. Phys.* **2013**, *138*, 12A535.
27. Finnis, M.W.; Sinclair, J.E. A Simple Empirical *N*-Body Potential for Transition Metals. *Pilos. Mag. A* **1984**, *50*, 45–55.
28. Sanchez, J.M.; Barefoot, J.R.; Jarrett, R.N.; Tien, J.K. Modeling of γ/γ' phase equilibrium in the Nickel-Aluminum system. *Acta Metall.* **1984**, *32*, 1519–1525.
29. Rosato, V.; Guillope, M.; Legrand, B. Thermodynamical and structural properties of f.c.c. transition metals using a simple tight-binding model. *Philos. Mag. A* **1989**, *59*, 321–336.
30. Shimono, M.; Onodera, H. Molecular dynamics study on structural relaxation of metallic glasses. *Mat. Sci. Forum* **2010**, *638–642*, 1648–1652.
31. Inoue, A. High strength bulk amorphous alloys with low critical cooling rates. *Mater. Trans. JIM* **1995**, *36*, 866–875.
32. Andersen, H.C. Molecular dynamics simulations at constant pressure and/or temperature. *J. Chem. Phys.* **1980**, *72*, 2384–2393.
33. Shimono, M.; Onodera, H. Geometrical and chemical factors in the glass-forming ability. *Scripta Mater.* **2001**, *44*, 1595–1598.
34. Shimono, M.; Onodera, H. Structural Relaxation in Supercooled Liquids. *Mater. Trans.* **2005**, *46*, 2830–2837.
35. Shimono, M.; Onodera, H. Icosahedral symmetry, fragility and stability of supercooled liquid state of metallic glasses. *Rev. Métallurgie* **2012**, *109*, 41–46.
36. Ohkubo, T.; Kai, H.; Hirotsu, Y. Structural modeling of Pd–Si and Fe–Zr–B amorphous alloys based on the microphase separation model. *Mater. Sci. Eng. A* **2001**, *304–306*, 300–304.
37. Park, J.; Shibutani, Y. Weighted Voronoi tessellation technique for internal structure of metallic glasses. *Intermetallics* **2007**, *15*, 187–192.
38. Hansen, J.P.; McDonald, I.R. *Theory of Simple Liquids*, 3rd ed.; Academic Press: New York, NY, USA, 2006.

39. Miracle, D.B. The efficient cluster packing model—An atomic structural model for metallic glasses. *Acta Mater.* **2006**, *54*, 4317–4336.
40. Hopkins, A.B.; Stillinger, F.H.; Torquato, S. Densest local sphere-packing diversity. II. Application to three dimensions. *Phys. Rev. E* **2011**, *83*, 011304.
41. Regge, T. General relativity without coordinates. *Nuovo Cimento* **1961**, *19*, 558–571.
42. Nelson, D.R. Order, frustration, and defects in liquids and glasses. *Phys. Rev. B* **1983**, *28*, 5515–5535.

© 2015 by the authors; licensee MDPI, Basel, Switzerland. This article is an open access article distributed under the terms and conditions of the Creative Commons Attribution license (<http://creativecommons.org/licenses/by/4.0/>).